PLEISTOCENE SHALLOW BRAIDED OUTWASH

NEAR GALT

PLEISTOCENE SHALLOW BRAIDED OUTWASH NEAR GALT

By

P.L. BOURQUE

A Thesis

Submitted to the Department of Geology

in Partial Fulfilment of the Requirements

for the Degree

Bachelor of Science

McMaster University

May 1973

ABSTRACT

A gravel pit west of Galt exposed about 6m of shallow braided outwash gravels which overlie deposits of unknown origin with eroded topography. The outwash shows two cycles of coarse sediment deposition with a relatively quiet period between. The lower cycle fines upwards from coarse gravel, through cross-bedded pebbly sand, to silty ripple-drift. The upper cycle erodes the silty sand and coarsens upwards from pebbly sand cross-beds to cobble gravel of longitudinal bars. These bars can be shown by their internal sandy horizons and stoss side sandy deposits to have grown by deposition at their upstream end.

The two major depositional cycles are related to north-westward flowing meltwater from the glacier as it stood at the Paris and Galt moraines respectively with the quiet period representing the time of retreat between the moraines. Subsequent melting to the north initiated an ice-contact spillway which ended the outwash deposition west of Galt.

ACKNOWLEDGEMENTS

The author wishes fo thank his supervisor, Dr. R.G. Walker for his assistance, particularly criticism, throughout this study.

In addition, George Eynon suggested the subject area and Jack Warwick furnished valuable technical assistance with the photography.

TABLE OF CONTENTS

LIST OF FIGURES

LIST OF TABLES

INTRODUCTION

The study of certain modern environments can be hindered in varying degrees by inaccessibility. An outstanding example of this is the study of modern turbidites, as their presence on the sea floor presents certain problems to the field geologist. Those wishing to study deposition in modern alluvial environments also face a problem with water, although admittantly not of the same magnitude.

The study of braided stream environments is hindered by the presence of water and/or by the coarseness of the sediments. The water level sets a limit to the depth to which one can excavate bedforms in safety and therefore sets a lower limit to the thickness of beds that can be studied. In addition, the turbulent nature of the flow at high discharge makes it impossible in most cases to study the processes of bedform development while it is forming. The coarseness of most deposits makes it most difficult to excavate study trenches when this is possible because of low water level.

In order to study vertical profiles to more than surficial depths it is necessary to turn to the geologic record. The local Pleistocene deposits, because of their proximity and ease of study since they can usually be excavated, are a logical choice since certain of them are

braided outwash deposits. Eynon (1972), studying Pleistocene deposits near Paris Ontario, was successful in adding understanding to the present braided stream model.

In this thesis the author studies Pleistocene braided stream deposits west of Cambridge (Galt) in what was described as a shallow braided system (Eynon, 1972, personal communication). Deposits found at one pit exposure will be discussed in light of our present knowledge of braided stream processes.

THE LITERATURE

Leopold and Wolman (1957) presented what has become a classic paper describing the principal river channel patterns. They distinguished three main patterns: straight, meandering and braided. The straight channel is the least common type, extends for only a short distance, and is bound at either end by either meandering or braided reaches. Meandering channels are characterized by having a single channel which repeatedly swings from one side to the other of the mean flow direction.

Braided rivers show successive division and rejoining of segments around alluvial islands. They are characterized by wide channels, rapid shifting of bed materials and continuous shifting of the position of the river course. They can exist in either coarse or fine material and be either deep or shallow systems.

Braided rivers in finer material (mainly sand) have been studied by Smith (1970) and Collinson (1970). The former worked on the Platte River which is relatively shallow (one metre or less). He showed that there, transverse bars are the main bedform and that braiding is effected by dissection of these bars. Collinson studied the relatively deep Tana River, Norway. In this river, the

dominant bedform is the linguoid bar although the larger islands and sidebars put the overall aspect of the river on a much larger scale. Both the Platte and Tana Rivers occupy distal portions of their respective drainage basins.

Braided rivers in coarse material have been the subject of research by a number of authors. Fahnestock (1963) studied the White River -- a proglacial stream, Williams and Rust (1969) and Rust (1972) studied the Donjek River, Alaska, and Krigstrom (1962) published a detailed paper on bar development on a number of valley sandurs in Sweden. All of these papers describe the stream morphology but, in addition, Williams and Rust, and Rust proposed facies which fit the morphologic features and could be used in studying the geologic record.

Working in Pleistocene deposits near Paris, Ontario, Eynon (1972) distinguished between "shallow braided stream facies" which blanket the entire system at the East Paris pit, and the underlying braided spillway system which has much larger structures (several metres in height). The shallow facies grades upward from the underlying coarse Bar Top facies. Both facies have imbricated gravels and sand lenses but the shallow system is generally sandier.

Four subfacies were recognized in the shallow braided stream facies. One is the final infilling of former channels by trough cross-bedded gravels which are

20 to 35cm thick and 0.75 to 4.15m wide. Another is imbricated pebble gravels with crude horizontal stratification. Thick (3m) accumulations are similar to Smith's (1970) longitudinal bars and Facies F of Williams and Rust (1969). Thin (10 to 20cm) accumulations overlie tabular cross-bedded gravels which are 25 to 40cm thick. Except for grain size these appear similar to the transverse bars described by Smith (1970). Finally, there are four forms of sand bodies. These are: sand-matrix-rich horizons within the thick imbricated gravels, planar laminated thin sandy horizons, cross-bedded lenses wnich are concave upwards, and a sandy capping over the whole sequence.

Eynon (1972) described the underlying outwash in considerably more detail and paid particular attention to the facies related to bar development. Three facies compose the longitudinal bar and these are the Bar Front, the Bar Stoss-Side and the Bar Top facies. The Bar Front facies consists of gravel to cobble size and forms large scale cross-strata from 4 to 6m high. These are developed downstream from the bar core -- a previously formed topographic high. The Bar Stoss-side facies consists of coarsening-upwards cross-bedded sandy gravels developed on the upstream side of the Bar Core. The Bar Top facies caps the earlier features. It consists of crudely horizontally stratified pebble gravels with some cobbles and, except for particle size, is very similar to the imbricate gravels of the

shallow braided stream facies. From the photolog with his thesis (Eynon, 1972) this facies appears to be several metres thick.

The Bar Top facies appears to be equivalent to Facies G of Williams and Rust (1969) and to form part of Facies 6 of Rust (1972) who combined Facies F and G of the previous paper. Williams and Rust explicitly note that Facies G is transitional to Facies F and Eynon (1972, p.74) observed that the Bar Top facies grades into the shallow braided stream facies. This, along with the structural and grain size similarities, strongly suggests that Facies F of Williams and Rust and Eynon's shallow braided stream facies are the same. A furhter analogy with Eynon's observations might be a sandur surface where a "proximal zone" is characterized by deep (one to several metres), well-defined channels which grade into more numerous, wider and shallower, less well-defined channels of the "zone further downstream" (Krigstrom, 1962).

The method of bar growth from a previous topographic high (Eynon, 1972) is a new hypothesis in the literature to the knowledge of the writer. In the "classical" bar development hypothesis proposed by Leopold and Wolman (1957) bar growth is initiated when local flow incompetence results in a coarse lag being deposited and this acts as a locus for continued deposition (Leopold, Wolman and Miller, 1964).

In addition, bar growth did not take place at the upstream end of the developing bar (leopold et al., 1964). Both Eynon and Rust (1972) give evidence that some bars, at least, grow by accretion at their upstream ends and Rust further suggests that braided rivers with relatively fine bed material (for instance, those described by Coleman, 1969, and Chien, 1961) tend to follow Leopold and Wolman's model, while braided rivers with coarse bedloads do not. Church (1972, p. 90) gives further evidence for deposition at the upstream end of braid bars on a sandur on Baffin Island.

While bar stratigraphy has been the subject of many studies, channel deposits are usually mentioned only in passing. Eynon (1972) did devote one section to large scale channels and called the Side-channel facies. The facies consists of three types of sedimentary structures: trough cross-bedding in granule gravels and coarse sand, planar laminations, and ripple laminations in medium to very fine sand. The trough cross-bedding occurs in the lower, central portions of the channel (in cross section) and the ripple lamination caps the uppermost parts of the channel fill. Similar channel deposits for the fine portion are also reported by Williams and Rust (1969, Facies C_1) and Rust (1972, Facies 3).

SETTING

The outwash exposure chosen for study is an un-named pit located about two miles west of Galt on Concession XII 0.9 miles north of Roseville Road (see Figure 1). The pit is on the northern edge of a locally very flat area characterized by occasional kettles and stream erosional valleys. Immediately to the north and again one to two miles to the west the plain is truncated by Bowman Creek which flows north and east to the Grand River at Blair 1.2 miles away. Southwards the plain disappears against Wentworth Till and eastward the plain increases in relief and passes through a break in the Paris moraine to end against the Galt moraine.

Bedrock contours have been mapped by Karrow (1963). His work shows that bedrock elevation is relatively constant at 850 ±15 feet for at least a one mile radius around the pit site. Highs of 902 and 934 feet exist just west of Doon and under the north-western edge of Galt respectively; southward towards Ayr and eastward, the bedrock falls to less than 625 feet.

The bedrock under the pit is the Silurian Salina Formation. It is described as grey and greenish, thin and irregularly bedded, soft, calcareous and argillaceous shale

with interbedded brownish, hard, dense dolomite (Caley, 1941, p. 39). It is not exposed in the immediate area; the outcrops between Preston and Galt along the Grand River to the north consist of rocks of the Guelph Formation which lies immediately to the east.

No erosion has affected the top surface of the area since the Pleistocene. This is demonstrated by the presence of abundant fossil ice wedges cutting into the underlying structures from the top surface. All the wedges have a wide top end of fine, clay-rich material which quickly narrows to about 10cm or less within 1m of the top (see Figures 5 and 14). The lower "tail" may continue downwards as a plane of finer material or a plane of structural disturbance (see Figure 13). The "tail" was seen to extend downwards several metres and could pass unnoticed through coarse gravel to reappear in a lower sand unit. No such structures were seen to begin below the top surface or to have only the lower "tail" preserved.

Figure 1: Pleistocene geology west of Galt showing the location of the study outcrop (yellow) and the outwash gravel (red) west of the Galt moraine. After Karrow, 1963.

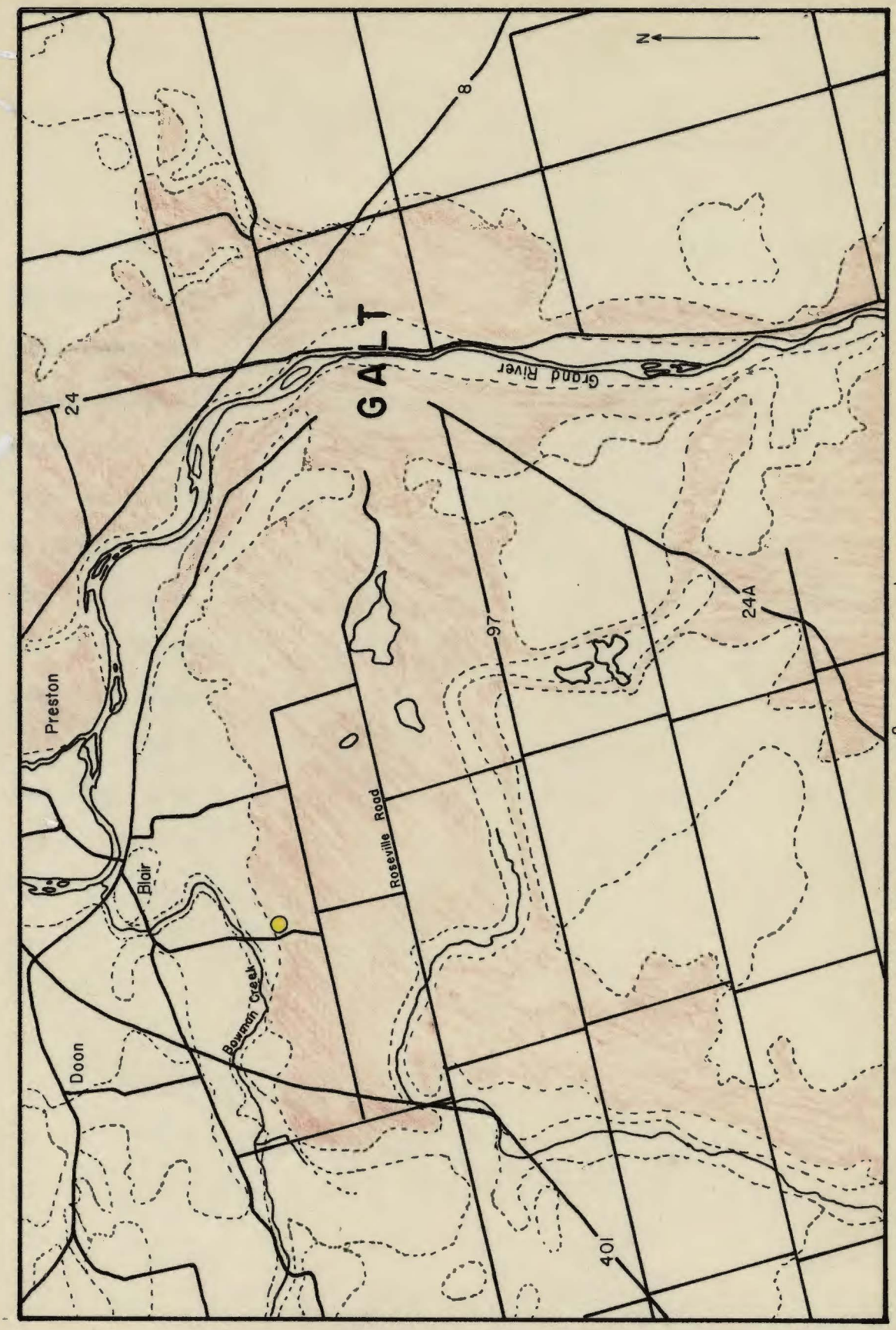
N
8
24
GALT
Grand River
97
24A
Roseville Road
Preston
Blair
Bowman Creek
Doon
401
0
miles

STRATIGRAPHY AND PLEISTOCENE HISTORY

Four major Glacials are recognized in the Pleistocene Succession of North America -- the Nebraskan, Kansan, Illinoian and Wisconsinan. The physiographical features of south-central Ontario are mainly the result of deposits or erosional forms of the Late Wisconsinan period and within this period the Wentworth ice advance and retreat most directly affected the study area. Eynon (1972) interprets the period of advance to be between 12,800 and 12,660 B.P. and the subsequent retreat to have occurred between 12,660 and 12,200 B.P.

The Wentworth ice advanced from the east and constructed the Paris, Galt and Moffat moraines from west to east respectively. With its retreat, large ice-marginal spillways down the Grand Valley developed which dissected the Paris moraine in the Galt area and both the Paris and Galt moraines south of Paris (Eynon, 1972, p.19) leaving remnant patches of Wentworth Till. This spillway system is thought to be the origin of the deposits studied by Eynon.

Figure 2 shows the writers interpretation of the north-south cross-section through the study area. It is interpreted from the map enclosures of Karrow (1963) with nomenclature modification after Karrow (1970). The depth

penetration of the various deposits are inferred and the cross-section is only intended to show the relative position of the units. The deposits directly above bedrock are unknown.

In the second paper, Karrow (1970) indicates that the till west of the Paris moraine, which he had formerly mapped as Wentworth Till, was actually different, and since he believed that it overlies the Port Stanley Till, he tentatively named it Port Stanley II. The division of the Port Stanley II and the Wentworth Till then lies along the western margin of the Paris moraine. However, since this moraine is dissected and overlain west and south of Galt, the exact extent of the two is unknown there and the deposits underlying the outwash gravel may be either.

The exposure at the pit can be divided into three units -- Lower, Middle, and Upper. Each is separated by a distinct break (see Figure 3).

The Lower unit could only be studied at two separate locations several metres north of the main outcrop and in a series of photographs. It is not known if it is part of the outwash system; the palaeocurrent is markedly different and the facies appear to be different from those above. The upper contact is erosional but not by the overlying bedforms of the Middle unit.

The Middle unit fines upwards from a cobble gravel to a metre thick accumulation of ripple-drift cross-laminated silty sand which prominantly crosses most of the outcrop face. Its upper surface is distinctly eroded by the Upper unit.

The Upper unit shows first a coarsening upward and then a fining upward trend, although it does not have the prominent silty sand beds -- its topmost beds are of coarse sand. This unit does show a number of wide, sandy, shallow channels and wedge shaped sandy deposits pointing downstream.

Figure 2: North-south cross-section through the studied exposure.

Key

6 Stream deposits.

5 Sand, shallow water lacustrine, kame and outwash.

4 Outwash gravel.

3 ? -- Wentworth Till or Port Stanley II.

2 Port Stanley II.

1 Silurian Salina Formation.

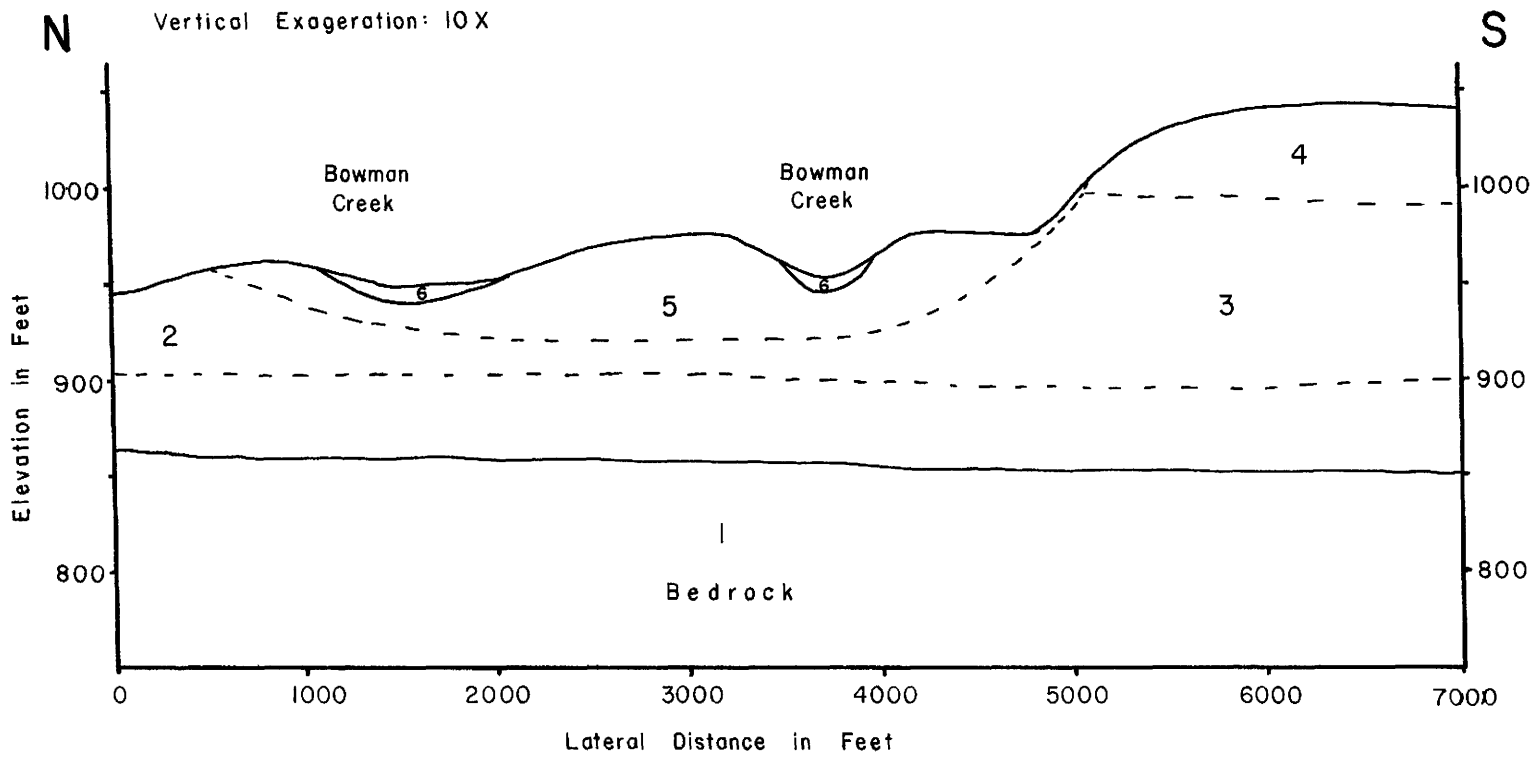
N
Vertical Exageration: 10 X
S
Bowman Creek
Bowman Creek
1000
900
800
Elevation in Feet
1
2
3
4
5
6
6
Bedrock
0
1000
2000
3000
4000
5000
6000
7000
Lateral Distance in Feet

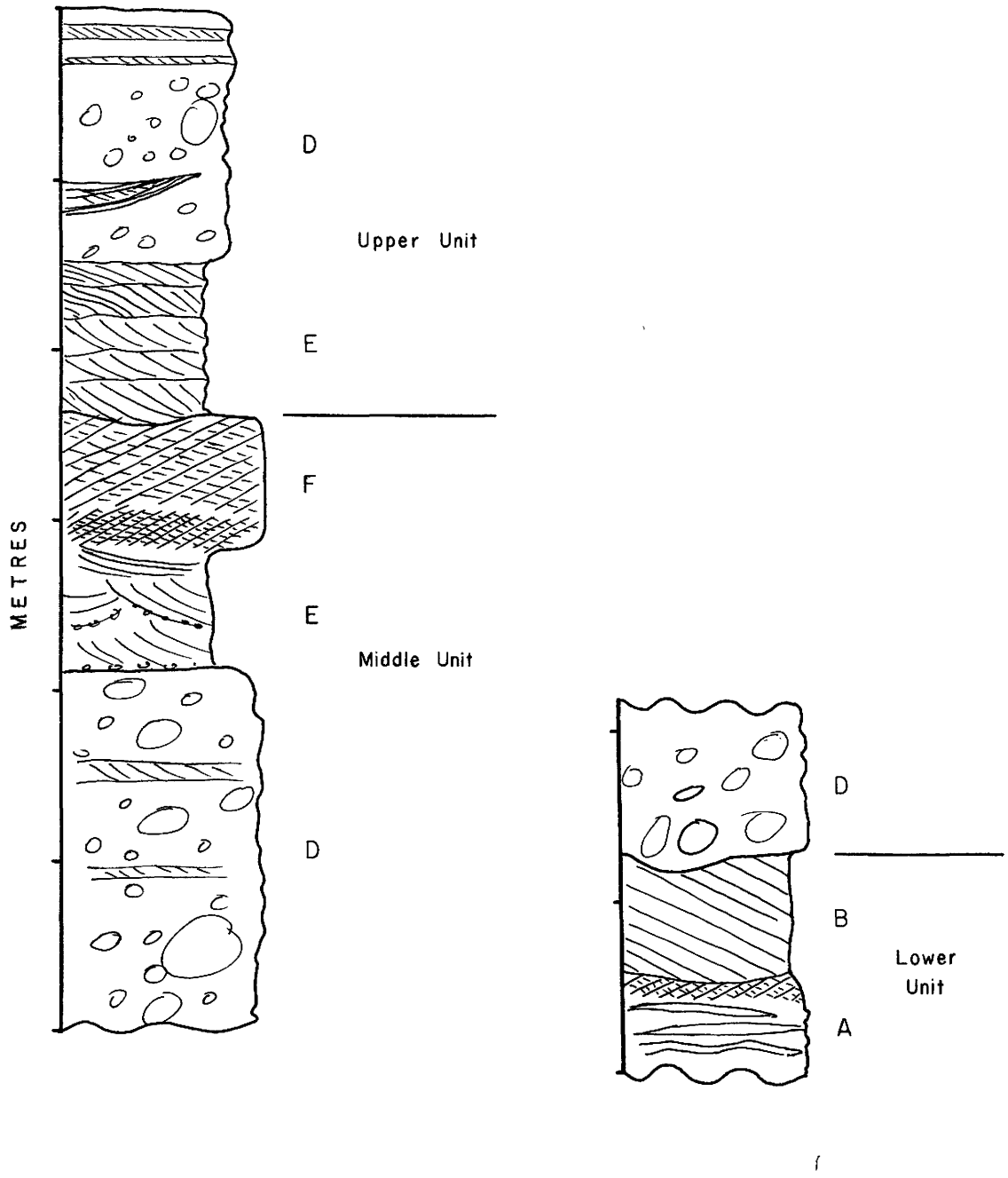

Figure 3: Schematic section through pit. The Upper and Middle units are for location 3 and the Lower unit is for location 9 (see Figure 4 for locations). The letters designate the respective facies which will be described later in the text.

THE EXPOSURE

This chapter will present diagrams and photographs which are intended to familiarize the reader with the overall aspects of the exposure.

Figure 4 is a plan view of the pit outcrop showing the relative position of the faces studied. The numbering will be used in the text and with photographs to locate features. Palaeocurrents for the Middle and Upper units are shown where they were recorded.

Figure 5 is a photograph of the face between point 5 and about half way between 5 and 1. The remaining outcrop towards 1 is very similar. Figures 6 and 7 show the east-west face between points 2 and 4 and between 5 and 6 respectively.

Previous to detailed study of the pit another face had existed along a line through points 8 and 9. Fortunately a sequence of photographs had been taken of it before it was excavated. One of these is shown in Figure 11 later in the text.

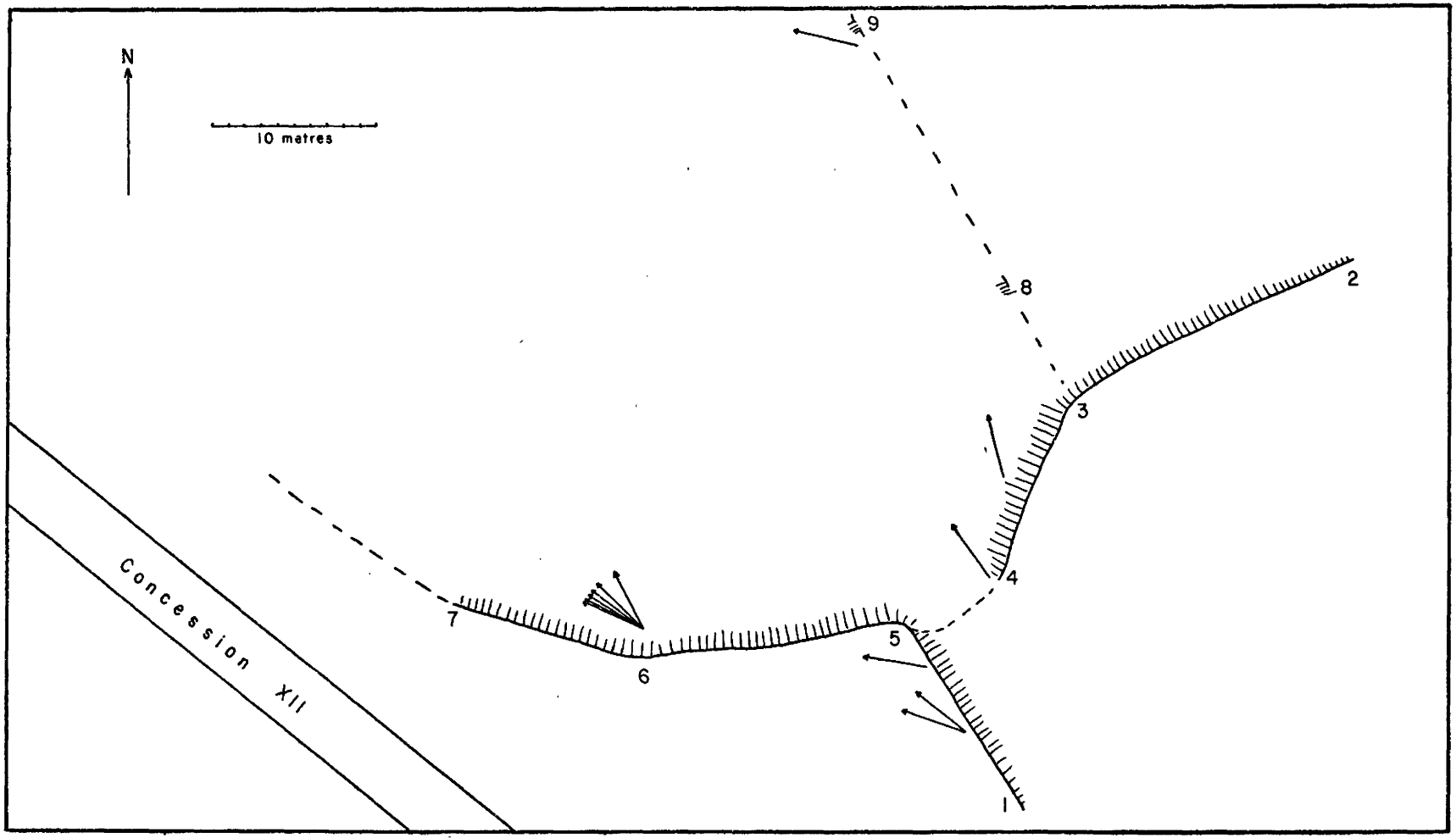

Figure 4: Plan view of the outwash exposure. The numbers mark locations and the arrows indicate palaeocurrent estimations for the Middle and Upper units.

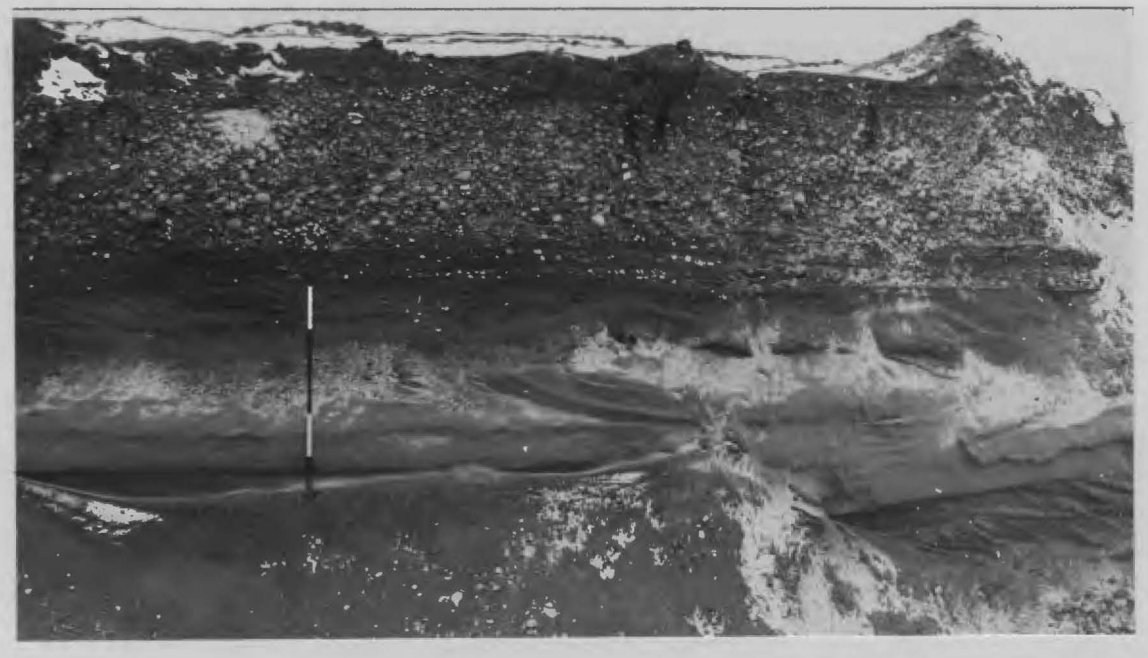

Figure 5: Photograph of the northern half of the north-south face south from point 5. The scale is in feet.

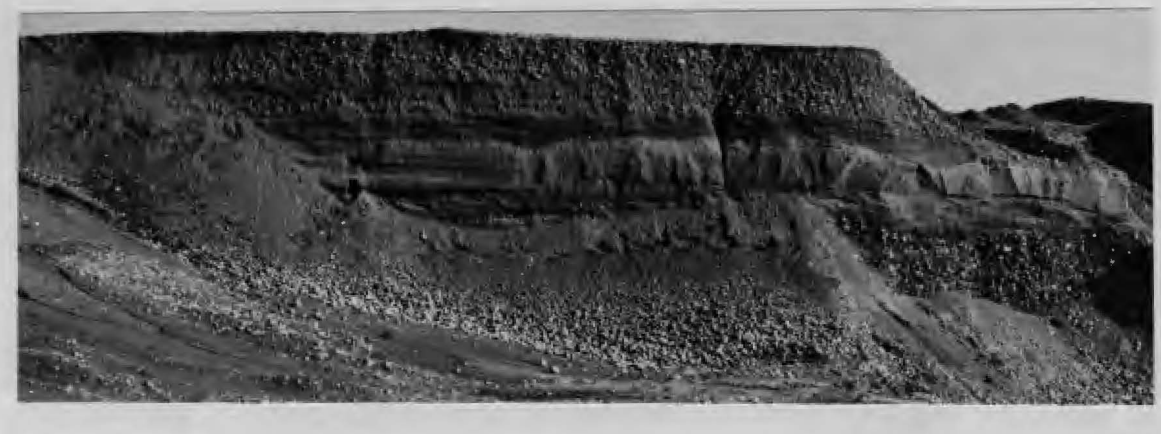

Figure 6: Photograph of the east-west face from points 2 to 4. The face is approximately perpendicular to palaeo-current. Scale is in feet.

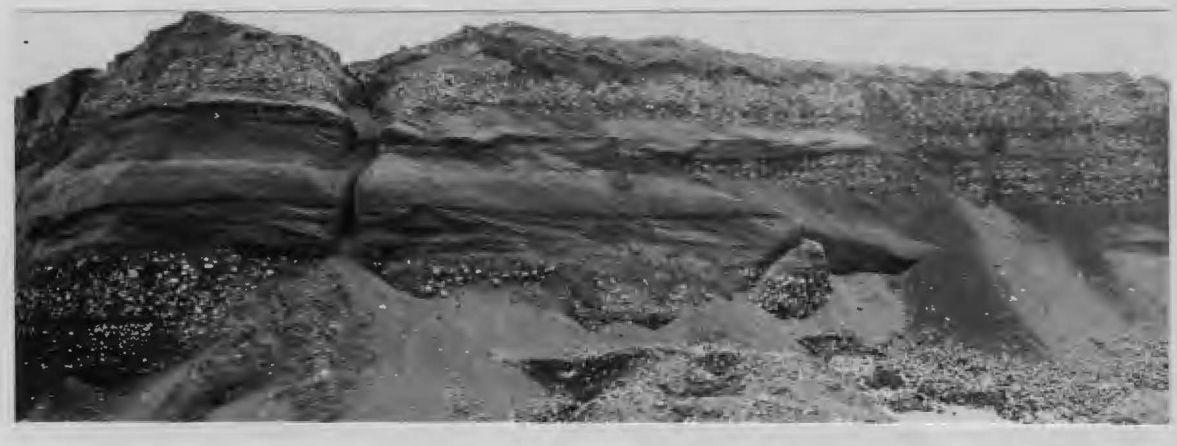

Figure 7: Photograph of the east-west face from points 5 to 6. The face is approximately perpendicular to palaeo-current.

INTRODUCTION TO THE FACIES

The facies are designated by letters and are chosen on the basis of structural and grain size similarities. They are:

Facies A: Alternating silty clay and silty sand.

Facies B: Low angle coarse sand laminations.

Facies C: Coarse gravel foresets.

Facies D: Coarse gravel with crude horizontal stratification.

Facies E: Cross-bedded sands and pebbly sands.

Facies F: Silty cross-laminations and ripple-drift cross-laminations.

To show the lateral extent and relationships of the facies, Figures 8 and 9 have been sketched from photographs. Figure 8 shows the units on the old face through points 8 and 9 and Figure 9 shows the east-west trending face from points 2 to 7.

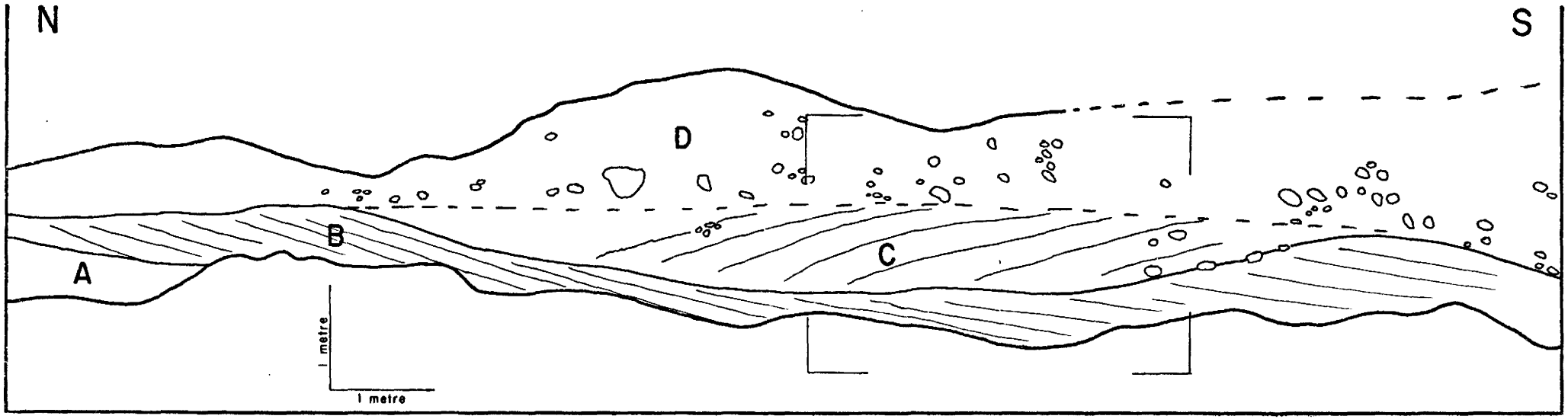

Figure 8: Sketch of the old face along a line through points 8 and 9. The letters refer to the facies described in the text. The photograph for the area within the rectangle is given in Figure 11.

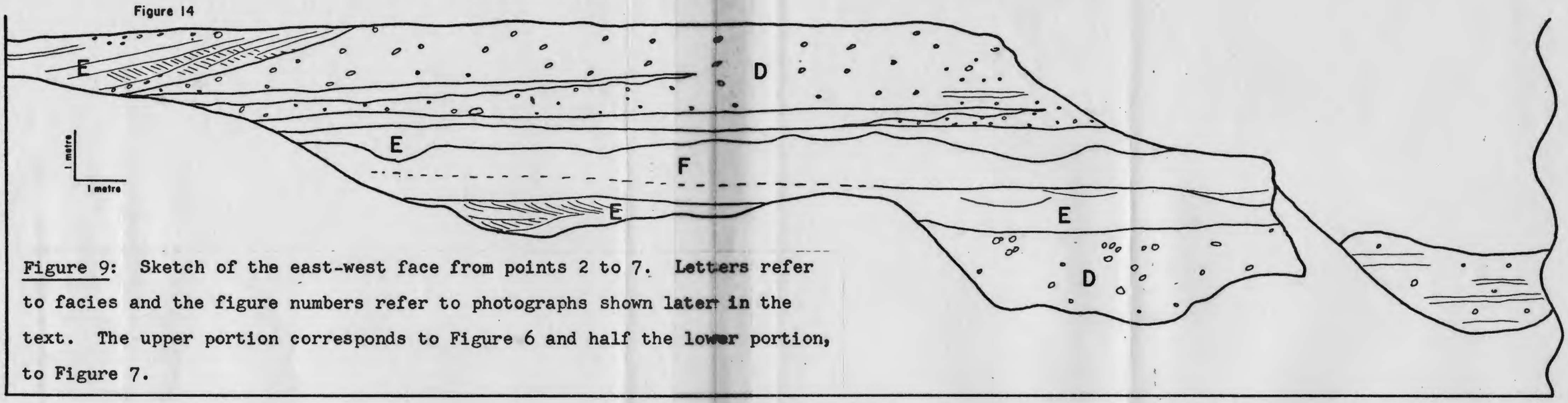

Figure 9: Sketch of the east-west face from points 2 to 7. Letters refer to facies and the figure numbers refer to photographs shown later in the text. The upper portion corresponds to Figure 6 and half the lower portion, to Figure 7.

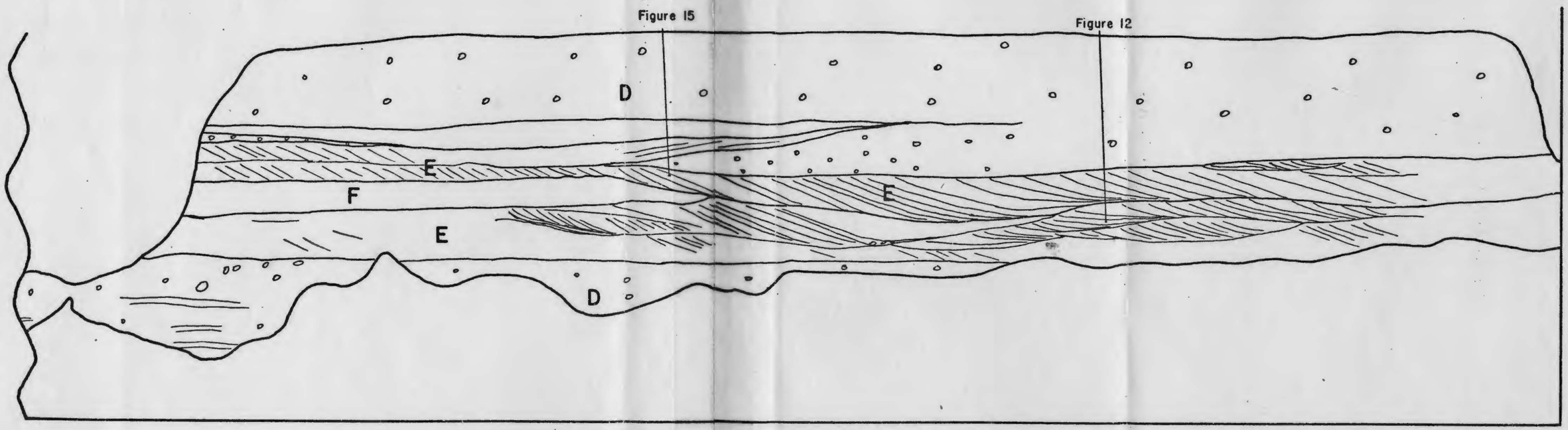

THE FACIES

Facies A: Alternating silty clay and silty sand.

This facies is the lowest observed in the sequence and could only be studied along the line of the old face at points 8 and 9. In addition, it can be seen at the northern-most end of the old face (seen in photographs and its position sketched in Figure 8). It is present at location 8 at least 0.5m above the lowest exposed gravel at point 3, and at location 9 at least another metre above 8. Hence its upper contact slopes downward from the north. This contact was seen at location 9 (Figure 12) and in the photographs of the old face and in both cases it is an erosional contact. At the latter location the minimum thickness of the unit is 0.6m.

The striking feature of the laminations is their distortion which has produced irregular lenses of clay-rich silt within silty sand. Figure 10 shows a moderately folded continuous bed of silty sand between clay-rich layers. The old exposure was much less regular since it was very difficult to trace individual beds. No distortion was observed at location 8.

The silty sand at location 8 consists mainly of

Type A cross-lamination (Jopling and Walker, 1968) with sets between 1 and 2.5cm thick, and preseved among these is a 4cm thick set of Type B ripple-drift cross-lamination. Palaeocurrent direction, as indicated by rib and furrow is 110°. Grain size analysis for this sand gives a median size of 3.7 phi and a silt content of 38%.

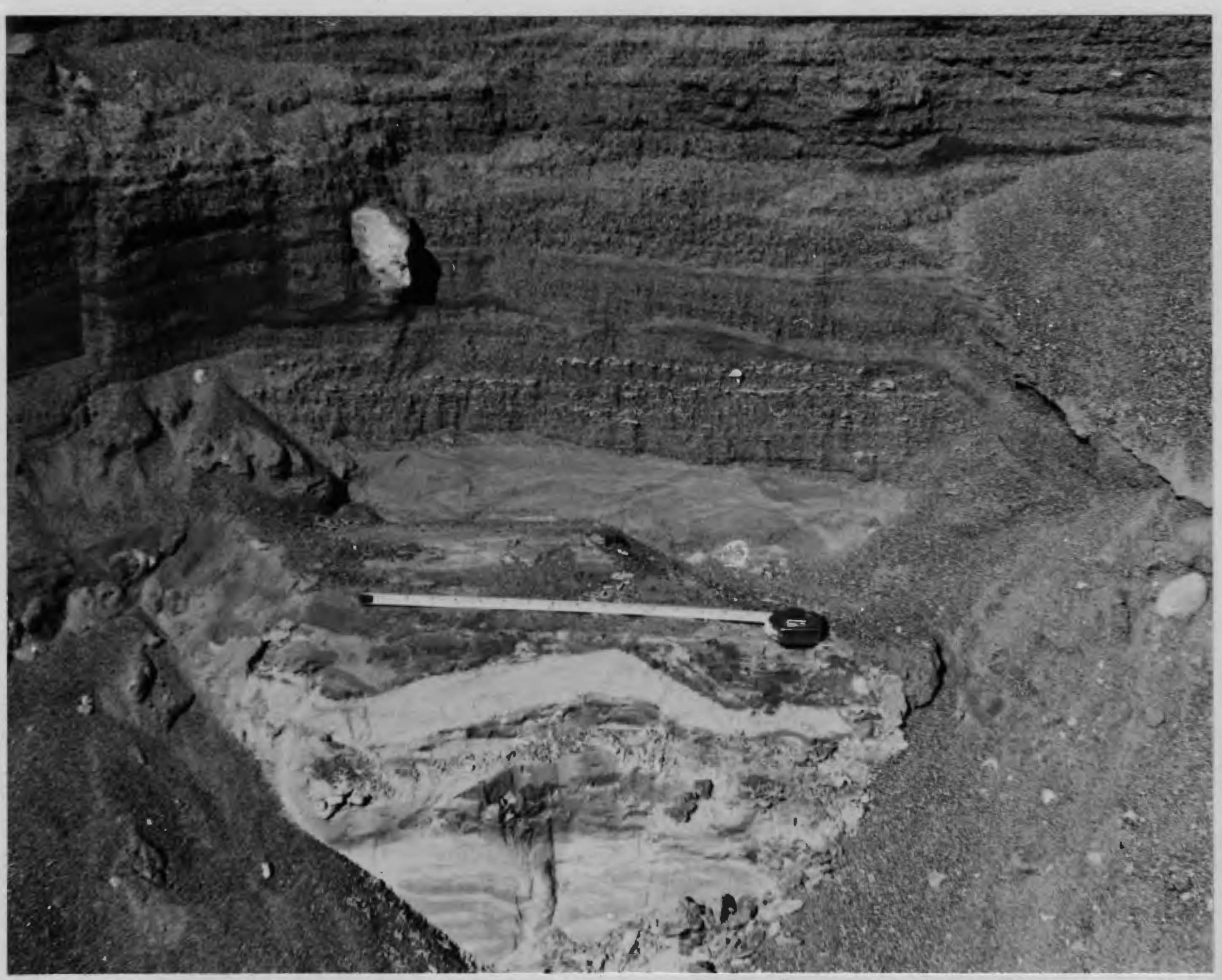

Figure 10: Photograph of the lower part of the outcrop at location 9 showing Facies A and B. Tape is in inches above and centimetres below.

Facies B: Low angle coarse sand laminae.

This facies might be considered to be part of Facies E, cross-bedded sands and gravels, but is described separately because of its relatively low dipping laminae, the inclusion of clay-rich lenses along the plane of the laminae, and its overall different relationship to other facies.

Like Facies A, this facies is only observed along the old face (see the upper portion of Figure 10 and the lower portion of Figure 11). However, it is continuous along the entire face. Presently it is only exposed at location 9 (Figure 10) where it is 0.7m thick.

Both its lower and upper contacts are erosional: the former seen in Figure 10 and the latter in Figures 8 and 11. The upper contact is especially noteworthy by virtue of its topography which varies as much as a metre from lowest to highest (see Figure 8) and the sharpness of the contact in view that the overlying sediments are considerably coarser.

The laminae are very continuous along the unit. They are 1.5 to 2cm thick and commonly show clay-rich portions (see Figures 10 and 11). Their orientation was calculated using the measurements from two mutually perpendicular vertical cuts and found to be dipping 22^{o} at 233^{o}.

Other features include a large blocky cobble of

dolomite about 10cm diameter located about 20cm from the bottom of the facies as seen in Figure 10. The laminae below the block are not disturbed and the laminae along its sides abut abruptly against it. Also, the lower 10cm of the unit is rich in clay chips aligned along the laminae orientation. The largest of these chips reaches 1cm in length and they appear very similar to the underlying silty clay(Figure 10).

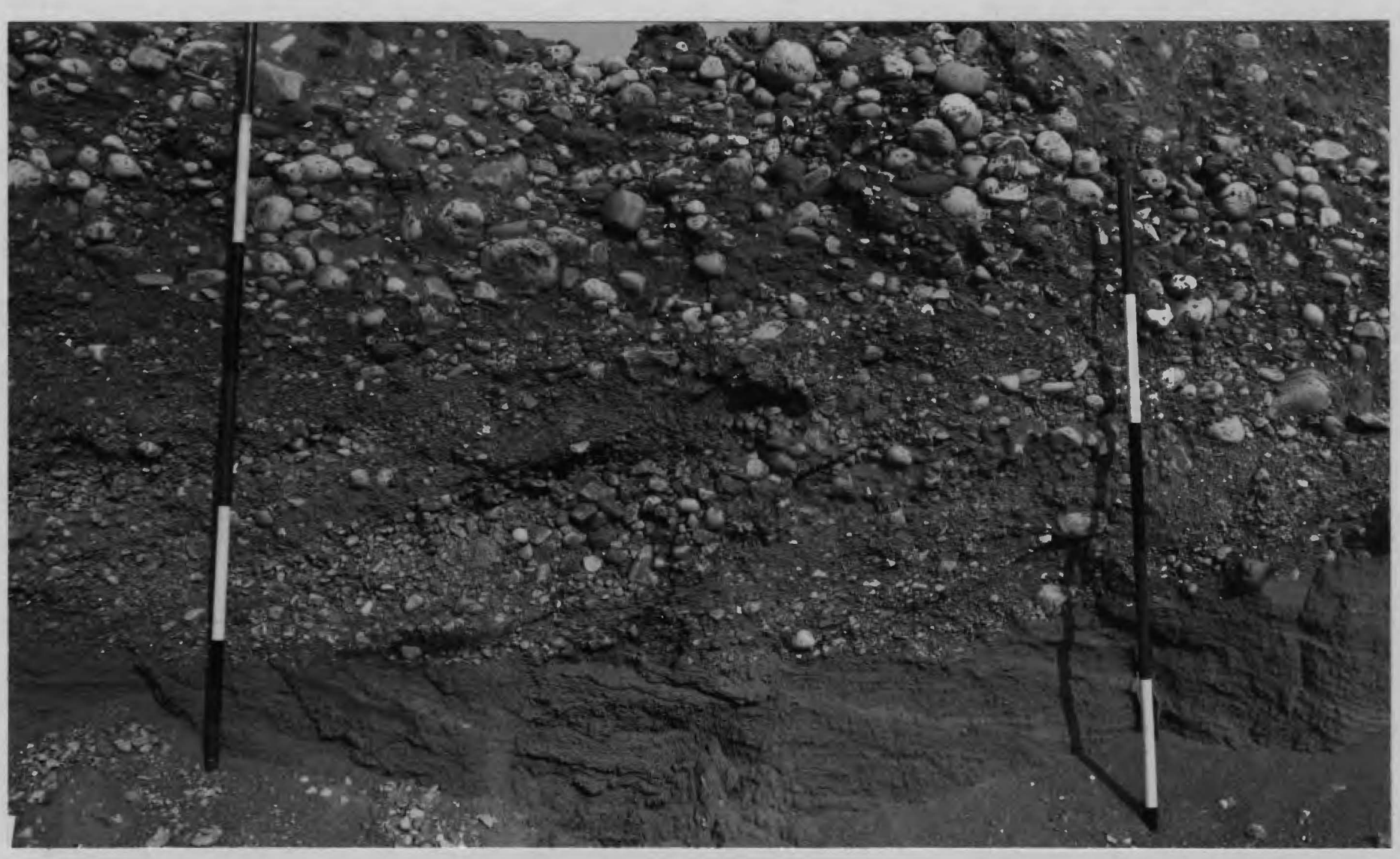

Figure 11: A photograph of Facies B, C and D along the old north-south face through locations 8 and 9. Scale is in feet.

Facies C: Coarse gravel foresets.

This facies is seen only in the photographs of the old face (see Figures 8 and 11). It is located between two topographic highs of Facies B below, which are about 9m apart, and since the face is approximately parallel to the general palaeocurrent, this length is probably representative of the downstream extent of the facies. The thickness is a function of the height of Facies B. The unit begins at the top of the upstream elevation and continues more or less in a straight line to pinch out against the top of the downstream high.

The foresets display an alternation of matrix free and matrix rich layers which dip at approximately 20^{o} at their maximum. They become asymptotic at both ends although the upper portions show more gradual rounding. At their upstream end the foresets vary from 10 to 16cm thick but thin to about 4cm at the downstream end.

Grain sizes show a change corresponding to the foreset thickness change. At the upstream end the matrix free zones are composed of pebbles of about -5.5 phi size while downstream these diminish to pebbles around -4 phi. Similarly, the matrix rich foresets change from a pebble gravel at the upstream end to what appears to be a granule gravel downstream. The ten largest clasts average 11.5cm -- cobbles. This size of clast is not common and is almost exclusively found at the upstream end -- especially along the lower contact of the facies.

Facies D: Coarse gravel with crude horizontal stratification.

This facies occurs at two horizons. The lower one (in the Middle unit) underlies the entire east-west face (see Figures 6 and 7) where it is at least 2m thick. It is also seen at location 9 where it is only about 0.5m thick and along the old face as seen in Figure 11. Where seen, the contact with the underlying Facies B of the Lower unit is always erosional, and the contact with Facies C, the coarse gravel foresets, is gradational. The top surface is horizontal and either gradational or slightly erosional.

The Upper occurrence, seen in Figures 5, 6, and 7, covers the entire outcrop area except at location 2. It is around 1m thick and differs from the lower occurance in enclosing larger, definitive channel-like sand bodies and wedge-like sand deposits. However, these features may be present in the lower occurrence but not exposed due to the relatively smaller outcrop area. The lower contact may be either erosional or gradational. Where it overlies sandy foresets (Figure 15), the contact is erosional, elsewhere it is gradational (Figure 5).

The horizontal stratification is imparted by sandy and sand-matrix-rich lenses and horizons. In the lower occurrence the lenses range from 10 to 20cm thick, from 1 to 3m wide perpendicular to flow, and at least (but probably more) 4m long parallel to flow. Parallel to flow their

thickness remains constant. Some of the lenses show cross-laminations consistent with palaeocurrent direction, while others show roughly horizontal or no stratification. The sandy lenses in the upper occurrence are similar except wider -- from 3 to 4m wide. Two tabular cross-bedded horizons near the top of the face (Figure 5) persist along the entire face (about 14m).

Several sandy horizons in the upper occurrence deserve special note. The horizons can be seen to the right in Figure 7 where they slope downwards to meet the lower contact of the coarse gravel. In addition, they are parallel to the overlying sandy wedge. This is discussed later.

Palaeocurrents were estimated from imbrication measurements and measurement of foreset orientation in one of the above mentioned tabular cross-bedded units. Results of the imbrication measurements are shown in Table 1. The foresets are dipping 31^{o} towards 342^{o} which is 34^{o} away from the imbrication measurement for this face.

In the lower occurrence the average diameter for the ten largest clasts from two areas is -7.5 and -7.6 phi and the largest clast seen "in situ" is 28cm wide (a boulder). In addition, at least one rounded boulder as large as 80cm in diameter was seen on the pit floor and it (plus others almost as large) is thought to have come from this unit. The ten largest cobbles from the upper unit as measured along face 1-5 average -6.9 phi.

Location	Number of Cobbles Measured	Range of Direction of dips of Long Axis	Vector Mean	Inferred Flow Direction	Vector Magnitude	Range of Dips	Average Dip
Lower occurrence Face 3-4	10	110-180	166	346	82%	15-33	24
Lower occurrence Location 9	9	080-125	114	294	98%	16-38	26
Upper occurrence	19	105-180	128	308	94%	8-51	33

Table 1: Results of imbrication measurements for Facies D.

Facies E: Cross-bedded sands and pebbly sands.

This facies has three main occurrences. In the Middle unit it occurs everywhere directly above the cobble gravel beds and below Facies F, the silty sand, where it is present. Where Facies F is not present (between points 6 and 7) this occurrence lies directly below the erosional contact between the Middle and Upper units. The second occurrence lies in the Upper unit directly above the erosional contact. It scours both Facies F and the lower occurrence of Facies E where Facies F is absent. Finally, Facies E occurs in wedges within the upper cobble gravel (Facies D).

The Middle Unit:

In the Middle unit, Facies E has a partly erosional, partly gradational contact with the underlying gravel of Facies D and a gradational contact with the overlying Facies F. Where Facies F is absent (between points 6 and 7) the contact with the Upper unit Facies E is erosional. Its thickness varies from 0.3 to 0.8m depending upon both the upper and lower contacts and it occurs everywhere where the appropriate section is exposed.

In the eastern parts of the exposure, Facies E consists of pebbly sand trough cross-beds from 15 to 25cm deep and 2 to 2.5m wide with laminae between 1.5 and 2cm thick. The base of the troughs are commonly marked with a pebble lag (see the lower right corner of Figure 5).

Towards the west these grade into tabular cross-laminations. These occur in cosets of two to four, but usually three, sets which range in thickness from 15 to 45cm with an average thickness of 30cm (9 measurements). The lower foreset contact ranges from angular to asymptotic with the lowest set tending to be angular and the upper, asymptotic.

A common feature is aggrading toesets (see Figure 12). These represent thick accumulations of toesets which can attain half the thickness of the whole set; the thickest measured was 20cm (Figure 12). The accumulations occur on the upstream end of an underlying dune stoss side and always include pebbles, at least in the lowest toesets. One example showed pebbly sand 5 to 7cm thick grading upwards into a thick lens of fine silty sand (sample SN1).

One example of reactivation of dune was observed. This is recorded in the lower part of Figure 15.

Five palaeocurrent orientations were obtained from the tabular sets near the area of the photograph in Figure 12. Four were measured by making two mutually perpendicular vertical cuts in each set, and the fifth was obtained from the foreset strike. The results are tabulated in Table 2.

Table 3 lists the results of grain size analysis. The first three samples represent "normal" pebbly coarse sand troughs within the unit. They are bimodal and are moderately to poorly sorted. Samples SD3 and SD4 both represent an intermediate grain size between Facies E and F;

both come from just below the ripple-drift cross-laminated unit, and while the sorting is still moderate to poor, both samples are unimodal. Samples SN1 and SN2 were taken from a foreset cross-laminated set. The coarser sample (SN2) grades quickly into the silty sand in the manner of aggrading toesets as described above. Both these samples are unimodal and are moderately sorted.

Table 2: Palaeocurrent estimations from the cross-beds of the lower occurrence of Facies E (part of the Middle unit).

Where Measured	What Measured	Current Azimuth	Foreset Dip
Location 6 Uppermost set	foreset plane	314	40
Location 6 Uppermost set	foreset strike	307	
Location 6 Next-to-top set	foreset plane	332	34
Location 6 Next-to-bottom set	foreset plane	297	29
Location 6 Bottom set	foreset plane	302	30

	Sample Number	Mean	Coarse Mode	Fine Mode	Standard Deviation	Skewness	Percent Silt
"Normal" Troughs	SC1	0.63	-2.5	0.75	1.10	-0.07	.9
	SC2	0.86	-3.0	1.0	0.91	0.17	1.0
	SC3	0.55	-3.5	0.75	1.31	-0.20	.6
Transition Zone	SD3	1.53		1.5	0.80	0.12	.9
	SE4	1.83		2.5	1.13	0.07	4.8
Foresets	SN1	3.10		3.0	0.68	0.29	10.7
	SN2	0.87		1.0	0.76	0.31	.8

Table 3: Results of grain size analyses for the samples of the lower occurrence of Facies E (within the Middle unit). Units are phi sizes and the statistics were obtained using standard Folk and Ward (1957) methods. Sample locations are given on the next page.

Table 3 (continued):

Location from which samples were taken.

SC1: Lowest set at location 4 (trough).

SC2: Highest set at location 4 (trough).

SC3: From a trough between points 2 and 3.

SD3: From just below Facies F from low angle parallel laminations. (See left side of Figure 5)

SE4: From along the bottom of Facies F between points 2 and 3.

SN1: From the silty sand aggrading toeset lens (see text).

SN2: From the foreset laminations immediately upstream of sample SN1 (into which it grades).

Figure 12: Photograph taken between points 6 and 7 showing the upper and lower occurrences of both Facies E (the cross-beds) and Facies D (the gravel). The horizontal lines at the sides mark the contact between the Upper and Middle units. Note the aggrading toesets in the centre of the picture. Scale is in feet.

The Upper unit:

Facies E lies everywhere at the base of the Upper unit and its lower contact is always erosional. Its upper contact is variable. Along the face between points 1 and 5 Facies E grades upward into the cobble gravel (Figure 5) while along the east-west face, the contact with the overlying gravel or wedge forms is sharp (see Figure 12). Overall thickness varies from 10 to 100cm depending upon the lower surface -- the greatest thicknesses occur where the lower unit has been most deeply scoured or is topographically lower as is the case to the west (between points 6 and 7).

This occurrence appears to consist entirely of tabular cross-bedded sets which vary in thickness from 10 to 100cm. Usually only one or two sets are present but four were seen along face 1-5 (Figure 5). The thinner sets are generally found at the eastern end of the outcrop while the thick sets (Figure 12) occur towards the west. Asymptotic foreset contacts are the rule with the most asymptotic occurring towards the west (downstream). Aggrading toesets are also present as in the Middle unit (see the left-hand side of Figure 12).

One example of a fully preserved dune-form was seen along face 1-5 which is approximately parallel to the palaeocurrent direction. This is recorded in Figure 13.

A similar feature was seen along face 2-3 where tabular cross-beds with truncated tops are overlain for several metres by 10cm of parallel laminations. Downstream these laminations bend downwards parallel to the upstream foresets to form a thicker tabular set of foresets.

Four palaeocurrent estimates were obtained. One was made from two flat pebbles lying on the foresets, and the other three were measured from two mutually perpendicular vertical cuts into the foresets. The locations and results are given in Table 4.

Seven samples from this occurrence were analysed and the results are shown in Table 5. The means range from very coarse to coarse sand, the inclusive standard deviation ranges from very poorly sorted to moderately sorted, and the inclusive graphic skewness, from strongly coarse-skewed to near-symmetrical. Most of the samples are bimodal. No consistent lateral of vertical trend could be discerned from the analyses except the fact of variability. However, field observation indicated that the foresets at the western end (the face between 6 and 7) contained noticeably smaller and fewer pebbles.

Table 4: Palaeocurrent estimations from foresets of the upper occurrence of Facies E (part of the Upper unit).

Where Measured	What Measured	Current Azimuth	Foreset Dip
Location 4	2 pebbles on foresets	325	20
Face 1-5	Foresets of dune-form	290	36
Face 1-5	Foreset plane	290	25
Location 6	Foreset plane	295	37

Table 5: Results of grain size analyses for the samples of the upper occurrence of Facies E (within the Upper unit). Units are phi sizes and the statistics were obtained using standard Folk and Ward (1957) methods. Sample locations are given on the next page.

Sample Number	Mean	Coarse Mode	Fine Mode	Standard Deviation	Skewness
SE1	0.39		0.5	0.88	-0.01
SE2-A	0.09	-3.5	0.5	1.17	-0.16
SE2-B	-0.24	-4.5	0.75	2.14	-0.43
SE3	0.77	-3.5	1.0	1.19	-0.18
SE5	0.95		1.5	0.93	0.01
SXX3	0.82	-3.5	1.0	0.74	0.01
SX1	-0.47	-4.0	0.5	1.97	-0.41

Table 5 (continued):

Location from which samples were taken.

SE1: Location 4. From the lower of two sets.

SE2-A: From face 2-3 (closer to 2).

SE2-B: From the lowest set above Facies F on face 1-5.

SE3: From the second from the top cross-bedded unit on face 1-5.

SE5: From the infilling of a scour into Facies F on face 2-3.

SXX3: From the dune-form (Figure 13) along face 1-5.

SX1: From the topmost set below the cobble gravel along face 1-5.

Figure 13: Photograph of the preserved dune-form along face 1-5 in Facies E of the Upper unit. Facies D is above in the photograph, Facies F is below.

Wedge-forms:

These features are only seen within the upper cobble gravel and at least four exist at this outcrop. Although they differ somewhat from each other in dimensions, they are alike in consisting mainly of sand and having the overall appearance of a wedge which always thins from the bottom and points towards the west. Unfortunately their position and the time of year made it impossible to study them close-up in any safety and therefore their description is mainly qualitative.

One example is found at location 2 at the top of the sequence which completely truncates the upper cobble gravel. Figure 14 shows this wedge along with the lower end of another immediately below. The larger wedge is at least 0.8m thick and greater than 7m long. It consists of pebbly sand arranged in parallel laminations dipping 10^{o} towards 53^{o}, as measured in the centre area, with sandy foresets climbing upwards in the opposite direction between the parallel laminations. All tend to converge towards the upper tip of the wedge. Three grain size analyses were performed on these sands and the results are shown in Table 6. The parallel laminations lower and farther into the wedge are decidedly bimodal but removal of the coarse mode from the analysis gives results very much like those of the other two samples (sample SY1-REV).

The wedge which is seen in the lower portion of

Figure 14 is only 25cm thick and is at least 6m long. It consists of pebbly sand in crude trough cross-sets. Two size analyses were performed (SW1 and SW2) and since the results were very similar, the values obtained are averaged. The mean size is -0.91 phi; the coarse mode, -4.5 phi; the fine mode, 0 phi; sorting, 2.08 phi; and skewness, -0.17 phi.

Part of another wedge can be seen in Figure 15 (upper sand). This wedge is very similar to the first described in that it consists of paralled laminations dipping into the wedge with foreset laminations climbing upwards between the parallel laminations towards the tip. In this case, however, nopebbles are present and the sand appears to be finer. The wedge is 35cm thick and around 8m long. An interesting feature is that its lower surface climbs upwards at the same angle as the sandy horizons in the cobble gravel immediately below. This can be clearly seen in Figure 7. Directly overlying the wedge and continuing downstream into the coarse gravel is a set of low angle, pebbly, coarse sand very similar to other sandy horizons within the gravel.

In every example where the top was seen, the upper contact of the wedge is sharp, and one contact had a thin (1cm) layer of clay between it and the overlying gravel. All have a sharp lower contact without signs of erosion and in three wedges the sandy tip continues westward for several metres into the coarse gravel.

Table 6: Results of grain size analyses for the samples from the large channel-like wedge at location 2. Units are phi sizes and the statistics were obtained using standard Folk and Ward (1957) methods.

Sample Number	Mean	Coarse Mode	Fine Mode	Standard Deviation	Skewness
SY1	.85	-3.5	2.0	1.73	-0.57
SY1-REV	1.40		2.0	.96	-0.27
SY2	1.01		1.0	.88	.07
SY3	1.79		2.0	.71	-0.04

Location from which the samples were taken.

SY1: From the parallel laminations 2m left of the ice wedge.

SY1-REV: The same as SY1 with the coarse mode removed.

SY2: From foreset laminations 0.6m left of the ice wedge.

SY3: From parallel laminations above the top of the staff in Figure 14.

Figure 14: Photograph at location 2 showing a large channel-like wedge cutting the upper cobble gravel. The eastern end of another such wedge is immediately below between 2½ and 3½ feet above the base of the staff. The scale is in feet.

Facies F: Silty cross-laminations and ripple-drift cross-laminations.

This facies can be seen as a prominent, 1m thick band cutting the east-west face roughly in half (see Figures 6 and 7) and forming the lowest unit of face 1-5 (Figure 5). Near location 6 it is abruptly and completely eroded by the overlying unit (see Figure 15) although the upward swing of the lower surface suggests that it was thinning out from below as well. Its upper surface is erosional at all locations but its lower contact may be either erosional or gradational. In Figure 15 it grades from a thin (1-2cm) layer of coarser sand laminae which have an erosional contact with the lower dune. Along face 3-4 it grades into coarser large scale troughs which are significantly finer than the underlying troughs. Just east of point 3 the lower part of the unit includes a layer of pebbles one to two pebbles thick which opens into a single gravel trough cross-bedded set -- all within the silty sand. It would appear that, in general, this facies followed the underlying unit quickly and gradationally.

The unit consists almost entirely of Type A (Jopling and Walker, 1968) ripple-drift although their sizes vary. Along face 1-5 the lower half of the unit consists of sets 2 to 2.5cm thick while the upper half abruptly changes to dunes of a transitional form between Types A and B from 5

to 6cm thick. This pattern was also observed along face 2-3 although a wedge of finer sand of unknown internal structure exists along the base to the east (see Figure 6). The Type A cross-laminations can be seen in the lower and left-hand portion of Figure 16.

The palaeocurrent was estimated from rib and furrow for the ripples just left of the "channel" seen in Figures 5 and 16. The direction was 280°.

Four grain size analyses were performed. The results are tabulated along with their locations in Table 7.

A curious feature in the unit is the "channel" seen in Figures 5 and 16. It is 0.5m deep and appears to be about 4m wide. Its contact with the lower ripples is erosional. The lower part of the infill shows parallel laminations grading into Type A ripple-drift cross-lamination (Jopling and Walker, 1968) which climb towards the centre of the channel. These grade upwards into Types B and C ripple-drift cross-lamination which, in turn, grade upwards again to Type B but trending in the opposite direction. The outer and upper portion of the infill consists of laminations which paralled the wall of the feature. These plunge at 29° towards 330°.

Table 7: Results of grain size analyses for the samples from Facies F.

Sample Number	Median	Coarsest Grain	Percent Silt
SD1	2.90phi	-1.0phi	9
SD2	3.55	0.5	30
SD4	2.92	0.0	9
SD5	3.43	-0.5	21

Sample Location

SD1: The lower half of the unit at location 4.

SD2: From the wedge shaped base portion of the unit along face 2-3. This is easily seen in Figure 6.

SD4: The lower portion of the unit along face 1-5.

SD5: The upper portion of the unit along face 1-5.

Figure 15: Photograph of the upper part of the face near location 6. Note the truncation of Facies F, the underlying reactivation surface, and the overlying sandy wedge.

Figure 16: A closeup photograph of the channel-form in Facies F along face 1-5. The hammer handle is 30cm long (including head).

INTERPRETATION AND DISCUSSION

Water velocity pattern.

An estimation of the original flow velocities can be obtained from the sand size distribution using the techniques outlined in Appendix C. Two velocities are obtained. One is the velocity required to move the coarsest one (approximately) percent and the other is the velocity required to suspend the coarsest grain which is in the suspension (or saltation) population (Visher, 1969). Under conditions of uniform flow over a complete range of grain size material, the two estimates should be approximately equal within the error inherent in the empirical nature of the equations. If they are equal, we may feel reasonably confident that the estimate is correct. If the two estimates are significantly different, two interpretations are possible depending upon which is larger. When the velocity required to move the coarsest one percent of the grains is larger, one can interpret that the coarser material was emplaced by a faster flow than was present when the finer material was deposited and that the two populations were subsequently mixed. When the velocity to suspend the coarsest suspended load is greater than that required to move the coarsest bedload, one can interpret

that the coarser material was not available for transport at the time.

In Figure 17, both velocities are plotted against their stratigraphic position for the Middle and Upper units. The plot prominantly shows the two major episodes of deposition with an intervening quiet period. The flow between the two extremes is marked by fluctuating flows in which some deposits are the result of both high and low velocity currents. This is particularly true of the upper occurrence of Facies E where the velocity required to move the coarsest bedload is consistently higher than that required to suspend the fines. The upper part of the lower occurrence if Facies E is marked by similar values of the two velocity calculations. This indicates that the supply of sediment and the current velocity were balanced to maintain an efficient system during this time.

The results are hardly surprising as consideration of bedforms and flow regimes (Simons et al, 1965) would lead one to the same main conclusions, except that these results quantify the data and give more insight into the amount of fluctuation. It also gives more confidence to the observation that the coarse and fine fractions were deposited separately in some places.

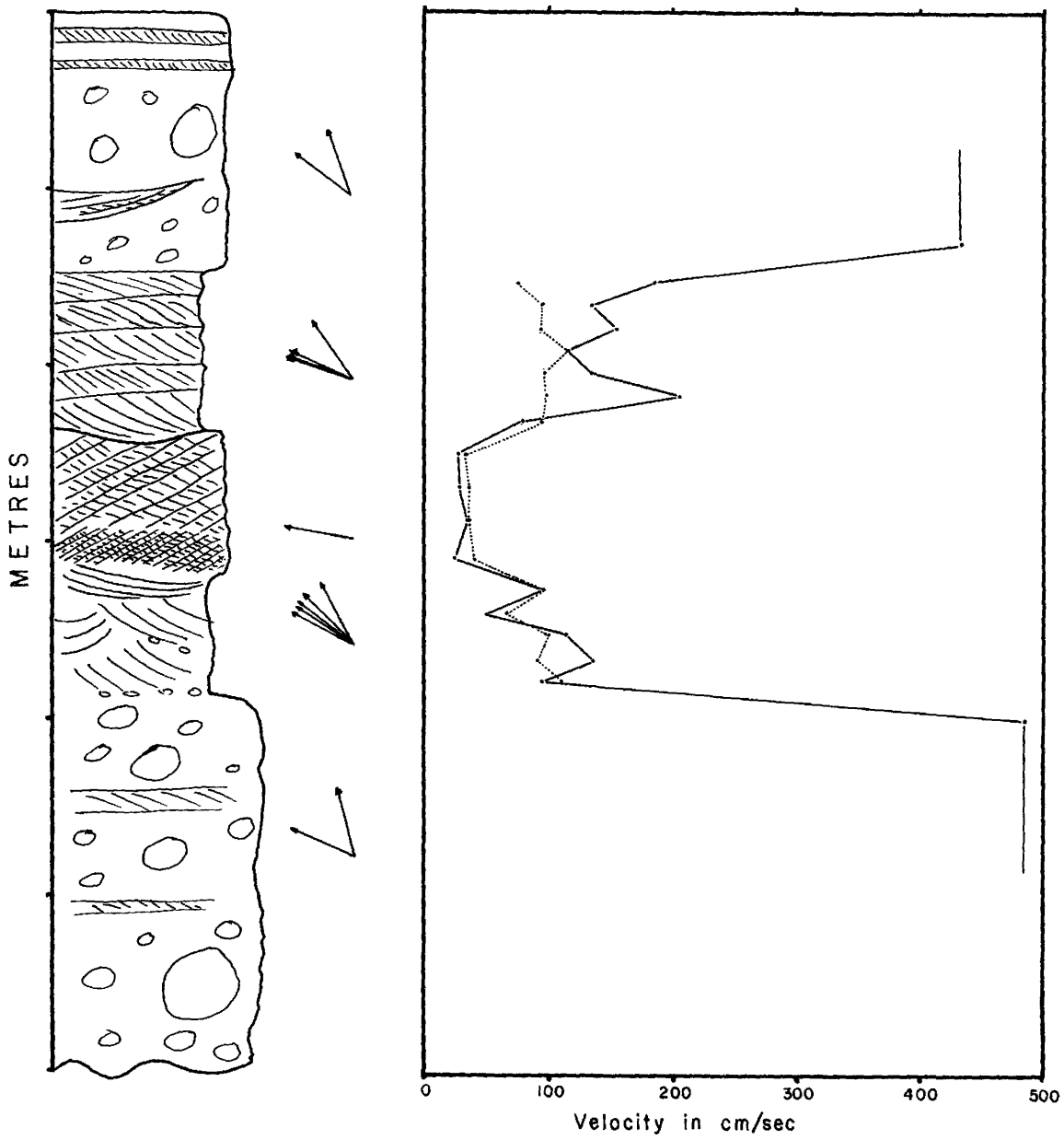

Figure 17: Comparison of velocity calculations and palaeo-current direction against stratigraphic position. The solid line in the graph is the velocity needed to roll the coarsest bedload and the dotted line is the velocity needed to suspend the coarsest suspended load. The arrows represent palaeo-current directions.

Palaeocurrent directions.

Palaeocurrent directions are indicated in Figures 4 and 17. The former shows the lateral distribution and the latter, the vertical distribution. Neither indicates any significant variation and the range of values (66^{o}) is relatively small and consistent with braided streams in general. Within this range there are two modes. The larger is about 300^{o} and the smaller, about 340^{o}. The grand vector mean is 308^{o} with a vector magnitude of 94%.

The Lower unit.

In function, the Lower unit is analogous to Eynon's (1972) Bar Core facies. No interpretation is attempted here regarding deposition except to suggest that it may have been close to the ice contact and is probably not directly associated with the outwash system.

The fact that Facies A is banded silt and clay and that its upper surface drops well over a metre towards the south gives some appreciation of a fair amount of erosion having occurred subsequent to deposition. In a similar manner, Facies B also underwent considerable erosion to produce the relief onto which the deposits of the Middle unit were lain. It would be interesting to know more about this "original" topography to ascertain its control on the overlying outwash gravels.

The Middle unit.

The Middle unit begins abruptly with the cobble gravels and subsequently fines upwards to the silty sand deposits of Facies F. The coarse gravels appear to be similar to those described by Williams and Rust (1969) as their Facies G. As such, it would represent a complex of longitudinal bars and low channels. It is also similar to Eynon's (1972) Bar Top facies but it does not overlie facies similar to his longitudinal bar. Facies C of this study looks similar to Eynon's Bar Front facies and builds forward from a topographic high. However, the other facies are absent and the foresets die out against the next topographic high.

The overlying Facies E appears to be similar to Facies 2 of Rust (1972) except that in the pit studied by the writer, trough cross-beds predominate in some areas -- the cross-strata described by Rust are mostly tabular. However, Rust's description aptly fits those cross-beds seen at the western end of the pit (Figure 12) which grade downstream from trough cross-beds. The change of preservation style from troughs to foresets may reflect a downstream decrease in stream energy or stream deepening.

The silty cross-laminated sands of Facies F is the equivalent of Rust's (1972) Facies 3 -- ripple-laminated silty sand.

All of the Middle unit, therefore, represents a

fining upward sequence from gravelly bars, through transverse bars, to the final silting up of the channel -- all due to a waning current.

The Upper unit.

The first sign of an increasing energy situation is the prominent erosional surface which produced an undulating surface upon the top sediments of the Middle unit. The first sediments of the new surge filled the erosional scours in a trough-like manner and then aggraded by the passage of transverse bars. Both the preserved dune forms and the increasingly asymptotic foreset contacts upwards attest to the increasing velocity and amount of sediment transport with time. The transition zone between low and high flow regimes is suggested by the low angle pebbly foresets immediately below the coarse gravel and above the dune form along face 1-5 (and seen in Figure 13). However, the two velocities of 184 and 75cm/sec for $\bar{U}$ and U_{10} respectively are not significantly different than velocities for other sets in this facies.

The initial pebbly sand cross-beds are followed by either cobbly gravel of by the "wedge" deposits. The cobbly gravel with its internal sandy horizons is interpreted to be low longitudinal bars, and the wedge-shaped sand bodies are the subsequent silting up of the upstream

portion of the channel a low water stage. The sand which extends downstream from along the top of the wedge becomes indistinguishable from other sandy horizons within the gravel.

If the sandy horizon which extends from the wedge tip represents the top of a bar, it can be argued that similar sandy horizons below the wedge represent former bar tops. As seen in the bar to the right in Figure 7, the fact that the lower sandy horizons all dip and meet with the lower contact of the gravel unit indicated that the bar grew by accretion to its upstream end, possibly in a manner similar to that proposed by Rust (1972, p. 243). Unfortunately, the downstream end of the bar could not be discerned.

It appears, then, that the coarse gravel along the top of the outcrop consists of a number of longitudinal bars. Periods of "normal" low stages result in a sandy horizon being deposited along the top of the bar by currents not capable of moving cobbles. When the stage drops lower than usual and remains low for some time, fine sands accumulate between the bars. These move up the stoss side of the bar with rising stages producing the wedge deposits, and as the current increases and begins to move over the bar again, coarser sands are added along the top of the wedge and bar deposits forming another sandy horizon within the bar.

The wedge deposits appear to be analogous to the Stoss Side facies of Eynon (1972). Both slope up the stoss side of the bar and appear to be deposited by water flowing over the top of the bar. In addition, Eynon also relates these deposits to lower than normal stages (page 87).

The top of the outcrop becomes sandier in a manner similar to the "sandy capping" described by Eynon (1972, p. 76). This is related to the final waning currents of the depositional sequence.

The ice sheet.

It is thought that the Middle and Upper units correlate with the glacial ice as it stood at the Paris and Galt moraines respectively. The water flowed directly off the glacier in a westward direction for several miles to produce the outwash gravel capping in this area. The quiet, silty period between the two units occured as the glacier retreated from the Paris to the Galt moraine.

There must not have been an ice contact, southward flowing spillway at the time which suggests that the ice to the north was either not melting substantially or its water emptied towards the west. The major southward flowing spillway developed later when ice to the north began to retreat. This effectively ended the outwash deposition west of Galt and produced the larger deposits to the south.

CONCLUDING REMARKS

The braid bars as described by Eynon (1972) were not found, but instead, the bars appeared to follow Rust's (1972) model by accretion at the upstream end. While the system studied is on a smaller scale than was Eynon's, several of his facies were observed in function at least. Both his Stoss Side and Bar Core facies were seen in the sandy wedges and the topography of Facies B respectively. Facies C of this study is also similar to Eynon's Bar Front facies.

It is felt that the wedge deposits should receive more attention to more clearly show their relationship with the sandy horizons within the bar gravel and their relationship with water stage in general. It would also be interesting to know if the two depositional episodes are in fact observed in other outcrops in the area and hence relate to general ice movement.

REFERENCES

BLATT, H., MIDDLETON, G.V., and MURRAY, R.C., 1972, Origins of sedimentary rocks: Prentice Hall, Englewood Cliffs, N.Y., 634p.

CALEY, J.F., 1941, Palaeozoic geology of the Brantford area, Ontario: Can. Dept. of Mines and Resources, memoir 226, 176p.

CHIEN, N., 1961, The braided stream of the lower Yellow River: Scientra Sinica, v. 10, p. 734-754.

CHURCH, M., 1972, Baffin Island sandurs: a study of Arctic fluvial processes: Geol. Survey Can., Bull. 216.

COLEMAN, J.M., 1969, Brahmaputra River: channel processes and sedimentation: Sedimentary Geol., v. 3, p. 129-239.

COLLINSON, J.D., 1970, Bedforms of the Tana River, Norway: Geografiska Ann., v. 52A, p. 31-56.

EYNON, G., 1972, The structure of braid bars: facies relationships of Pleistocene braided outwash deposits, Paris, Ontario: Unpub. M.S. Thesis, McMaster University, 235p.

FAHNESTOCK, R.K., 1963, Morphology and hydrology of a glacial stream, White River, Mt. Rainier, Wash.: U.S. Geol. Survey Prof. Paper 422A, 41p.

FOLK, R.L., and WARD, W.C., 1957, Brazos River bar: A study in the significance of grain size parameters: Jour. Sedimentary Petrology, v. 27, p. 3-26.

KARROW, P.F., 1963, Pleistocene geology of the Hamilton-Galt area: Ont. Dept. of Mines, Geol. Report 16, 68p.

———, 1970, Quartenary geology of the Stratford-Connestoga area, Ontario: Geol. Survey Can., Paper 70-34.

KRIGSTROM, A., 1962, Geomorphological studies of sandur plains and their braided rivers in Iceland: Geografiska Ann., v. 34, p. 328-346.

LEOPOLD, L.B., and WOLMAN, M.G., 1957, River channel patterns--braided, meandering, straight: U.S. Geol. Survey Prof. Paper 282B, p. 39-85.

LEOPOLD, L.B., WOLMAN, M.G., and MILLER, J.P., 1964, Fluvial processes in geomorphology: W.H. Freeman and Co., San Francisco, 522p.

MIDDLETON, G.V., 1965, editor, Primary sedimentary structures and their hydrodynamic interpretation: S.E.P.M., Special Pub. 12.

POTTER, P.E., and PETTIJOHN, F.J., 1963, Paleocurrents and basin analysis: Springer-verlay, Berlin.

RUST, B.R., 1972, Structure and process in a braided river: Sedimentology, v. 18, p. 221-245.

SIMONS, D.B., RICHARDSON, E.V., and NORDIN, C.F. Jr., 1965, Sedimentary structures generated by flow in alluvial channels: in G.V. Middleton, ed., Primary sedimentary structures and their hydrodynamic interpretation: S.E.P.M. Special Pub. 12, p. 34-52.

SMITH, N.D., 1970, The braided stream depositional environment: comparison of the Platte River with some Silurian clastic rocks, north-central Appalachians: Geol. Soc. Am. Bull., v. 81, p. 2993-3014.

VISHER, G.S., 1969, Grain size distributions and depositional processes: Jour. Sedimentary Petrology, v. 39, p. 1074-1106.

WILLIAMS, P.F., and RUST, B.R., 1969, The sedimentology of a braided river: Jour. Sedimentary Petrology, v. 39, p. 649-679.

APPENDIX A

Palaeocurrent Methods and Imbrication Data

Methods:

Since the field work was carried out during the winter months, the ground was frozen and excavation to determine palaeocurrent directions was very difficult to impossible. It was sometimes possible to cut a shallow trench with the pick end of a geologist's hammer. All measurements were made with a standard Brunton compass corrected for the 7^{o} westward declination of magnetic north from true north in this area.

Three principal features were used to estimate palaeocurrent depending upon the type of sediment. These are: imbrication in coarse gravels, orientation of foreset laminae, and rib and furrow.

Imbrication was measured in the coarse gravels of Facies D. At two locations the gravel was massive and the measurements covered an area less than a square metre. At the third location (face 3-4) measurements were made from several square metres between crude sandy horizons. Clasts were chosen which were obviously flattened (usually discoidal and within the same size range as the surrounding clasts.

For each set of data the vector mean and vector magnitude were calculated using the methods outlined in Potter and Pettijohn (1963, p. 264).

Three methods were used on different occasions to estimate the orientation of foresets and hence the current direction. The most commonly used method was to make a vertical, planar cut into the face so that the apparent dip of the foresets and the orientation of the new face could be measured. These, along with the same measurements on the exposed face, were subsequently plotted on a sterionet to obtain the true orientation of the foresets. A second method was to measure the strike of the foresets after having cut a horizontal plane along the top of the set. The current direction lies at 90° to the strike in the direction of foreset dip. This method does not give the foreset dip. Finally, on one occasion, the foreset orientation was estimated by measuring the orientation of two flat pebbles which lay along the foresets.

Rib and furrow is defined (Middleton, 1965) as "the expression on a bedding plane of small-scale trough cross-stratification." Their orientation is measured by cutting a horizontal plane through the cross-beds and measuring the direction in which the troughs open. This method was used with the cross-bedded silty sands.

Imbrication measurements -- raw data.

Lower Occurrence of Facies D Face 3-4		Lower Occurrence of Facies D Location 9		Upper Occurrence of Facies D Face 1-5	
Current Direction	Dip	Current Direction	Dip	Current Direction	Dip
350	33	300	23	320	22
355	15	280	19	325	47
010	20	260	38	295	19
335		290	27	0	49
025	24	290	30	290	35
060	23	280	25	300	17
310	18	290	16	325	18
290	33	305	22	300	37
330	30	290	32	345	36
330	22			315	51
				300	36
				285	38
				285	51
				310	45
				285	30
				315	8
				300	38
				305	20
				295	24

APPENDIX B

Grain Size Methods and Data

Method:

Taking samples from frozen pebbly sand presents certain problems, but what one loses by way of extra effort, one gains in the knowledge that a frozen chunk of sand contains an unbiased sampling of all grain sizes present -- none is lost over the edge of the shovel. Except with the silty cross-laminations, samples were always taken from a single cross-bedded set and from the middle region (vertically) of the set. The location along the set was chosen on the basis of its "average" appearance.

The samples were subsequently dried in an oven at temperatures between 50 and 60°C, split into samples 25 to 50 grams weight, and sieved using standard Tyler sieves at half phi intervals. Where samples contained only a small number of larger grains, the total sample was sieved for the coarser fraction and the finer fraction split and then sieved again. The resultant weights were weighted in the analysis to give their true proportion to the whole sample. The phi sizes of pebbles too large to fit in the sieves were determined by weighing and assuming a density of 2.7g/cc.

Folk and Ward statistics (1957) were calculated by computer using the author's own program written for this purpose. The relative percentiles are calculated by the program using a linear extrapolation between values; previous comparison of the results to that of hand calculated values showed the mean to be within ±0.03 phi, the sorting within ±0.05, and the skewness within ±0.07.

Grain size data:

All values are given in cumulative percents.

Facies E -- lower occurrence

	Sample Number						
phi	SC1	SC2	SD3	SD3	SE4	SN1	SN2
-4.0							
-3.5			4.44				
-3.0		2.10	6.42				
-2.5	2.59	2.73	7.69		.49		
-2.0	4.65	3.11	8.43		1.07		
-1.5	5.48	3.36	9.37		1.07		
-1.0	6.83	3.63	10.24	.09	1.19		.21
-0.5	11.03	5.13	13.21	.39	1.71		.99
0	23.17	13.18	22.99	1.59	3.30	.07	6.90
0.5	45.03	35.94	46.81	7.26	9.51	.20	32.55
1.0	65.23	61.41	72.53	24.24	23.51	.49	67.08
1.5	82.71	80.22	85.26	52.14	39.29	.98	84.53
2.0	92.20	87.90	92.57	70.68	56.25	2.56	88.54
2.5	95.59	93.59	96.81	88.45	73.97	18.66	93.00
3.0	97.40	96.93	98.50	96.05	85.50	53.11	96.96
3.5	98.40	98.24	99.08	98.24	91.45	74.97	98.49
4.0	99.11	98.98	99.42	99.10	95.24	89.29	99.19
Pan	100.00	100.00	100.00	100.00	100.00	100.00	100.00

Facies E -- upper occurrence

	Sample Number						
phi	SE1	SE2-A	SE2-B	SE3	SE5	SXX3	SX1
-5.0							
-4.5			7.58				
-4.0			9.53				8.54
-3.5		1.43	12.38	2.76		.98	11.09
-3.0	.42	2.66	14.30	4.14		.98	14.47
-2.5	1.04	4.47	16.89	6.02		1.51	18.66
-2.0	1.95	7.60	17.98	6.45	.27	2.09	22.25
-1.5	3.31	11.32	19.17	6.74	.95	2.57	26.00
-1.0	5.96	16.01	20.99	7.28	2.08	3.07	30.07
-0.5	14.18	25.21	25.96	9.26	5.75	4.50	36.12
0	30.88	42.49	36.70	16.74	14.66	10.38	46.36
0.5	55.25	65.63	53.60	37.05	31.70	31.07	61.68
1.0	77.52	81.85	69.71	61.30	52.58	60.05	76.24
1.5	91.72	92.38	83.00	82.40	74.95	84.40	89.31
2.0	95.88	96.36	89.93	91.86	87.12	93.53	94.90
2.5	97.86	97.83	95.35	95.67	95.34	96.97	97.35
3.0	98.80	98.50	97.76	97.27	98.21	98.44	98.20
3.5	99.22	98.86	98.46	97.99	98.98	98.95	98.61
4.0	99.43	99.16	98.88	98.60	99.31	99.24	98.95
Pan	100.00	100.00	100.00	100.00	100.00	100.00	100.00

Facies E -- "wedges"

	Sample Number					
phi	SY1	SY1-REV	SY2	SY3	SW1	SW2
-5.0						
-4.5					6.48	6.75
-4.0	2.35				8.38	8.02
-3.5	10.06				13.39	12.42
-3.0	11.75				17.38	16.18
-2.5	12.53	.88			21.91	19.18
-2.0	13.54	2.03	.16		28.31	23.18
-1.5	14.55	3.17	.37		34.91	28.41
-1.0	15.78	4.57	.91	.26	42.67	36.59
-0.5	17.62	6.65	3.09	.60	55.49	52.11
0	20.42	9.83	10.79	1.63	70.16	66.96
0.5	25.78	15.90	29.42	4.66	80.27	77.47
1.0	34.98	26.32	51.44	11.84	84.41	82.98
1.5	55.66	49.75	70.98	30.12	89.57	89.58
2.0	80.82	78.26	86.07	62.01	92.84	93.73
2.5	94.60	93.88	95.22	86.87	95.73	96.28
3.0	97.96	97.69	97.38	94.80	97.70	97.50
3.5	98.81	98.65	98.09	97.27	98.47	98.05
4.0	99.20	99.09	98.63	98.38	99.00	98.50
Pan	100.00	100.00	100.00	100.00	100.00	100.00

Facies A and F

	Sample Number				
phi	SA1	SD1	SD2	SD4	SD5
-1.5					
-1.0		.17			
-0.5		.22			.03
0	.01	.27		.02	.03
0.5	.03	.47	.01	.12	.07
1.0	.06	.79	.05	.42	.13
1.5	.15	1.11	.13	.77	.19
2.0	.40	2.83	.85	2.59	.46
2.5	1.33	19.22	7.39	21.29	4.36
3.0	12.30	55.33	25.97	54.65	25.22
3.5	38.21	77.69	47.85	77.12	55.00
4.0	61.61	90.75	70.67	90.64	79.46
Pan	100.00	100.00	100.00	100.00	100.00

Sample SA1 is from Facies A and the remaining samples are from Facies F.

APPENDIX C

Method and Results of Current Velocity Calculations

Two independent methods were used to estimate palaeocurrent velocities. The one method calculates the average current velocity needed to move (as bedload) the grain equal in size to the coarsest 1% of the distribution; this will be designated $\overline{U}_{cr}$. The other method calculates the current velocity needed to suspend the coarsest grain which is estimated to have been in suspension; this will be designated U_x where "x" is a number which is defined below. Both methods rely on data obtained from a grain size analysis of a sample taken from the area being studied. For each sample, the cumulative weight percent is plotted against phi sizes on probability paper.

To obtain $\overline{U}_{cr}$, the coarsest 1% size is read off the probability graph. This size is then converted to centimetres and the velocity calculated using Shield's diagram and associated formulae (see Blatt et al, 1972, p. 90).

The calculation of U_x involves the separation of the bedload from the saltation grain size populations (see Visher, 1969) on the probability graph. The break represents the coarsest grain which was held in suspension by the

moving water and its settling velocity can be obtained from Rouse's graph (see Blatt et al, 1972, p. 54). The upward component of current velocity is a function of relative roughness (see Blatt et al, 1972, p. 99). Generally this value lies between 2 and 4% of mean velocity, but in very turbulent water the value can attain 10%. This is doubled to approximate two standard deviations (95%0 and from this figure the current velocity can be estimated. The "x" referred to above is the percent of upward component assumed for the flow.

The table following gives the velocities and the grain sizes upon which the velocities were calculated. The roughness factor is also shown (as percent upward velocity). For the ripple-drift, normal roughness is assumed, and for all other situations, very turbulent conditions are assumed.

Velocity Estimations

Sample Number	Coarsest Bedload phi	Coarsest Suspension phi	Settling Velocity cm/sec	Upward Velocity %	$\bar{U}cr$ cm/sec	Ux cm/sec
Facies E -- lower occurrence						
SC1	-2.5	-0.64	22	10	93	110
SC2	-3.0	-0.54	20	10	111	100
SC3	-3.5	-0.32	18	10	133	90
SD3	-0.5	0.1	13	10	47	65
SE4	-2.5	-0.4	19	10	93	95
SN1	1.0	1.95	2.6	10	28	26
SN2	-0.6	-0.3	17	10	48	85
Facies E -- upper occurrence						
SE1	-3.0	-0.8	23	10	112	115
SE2-A	-3.5	-0.43	19	10	133	95
SE2-B	-4.5	-0.5	20	10	206	100
SE3	-3.5	-0.36	19	10	156	95
SE5	-2.0	-0.4	19	10	79	95
SXX3	-3.5	-0.3	19	10	133	95
SX1	-4.0	-0.1	15	10	184	75
Facies E -- wedges						
SY1	-4.0	0.84	7.2	10	158	36
SY2	-1.0	-1.7	38	10	56	190
SY3	-0.5	0.9	6.8	10	47	34
SW1	-4.5	-0.8	23	10	197	115
SW2	-4.5	-1.15	29	10	187	145
Facies F						
SD1	0.5	1.83	2.9	4	33	36
SD2	1.5	1.73	3.3	4	23	41
SD4	1.0	1.8	2.9	4	28	36
SD5	1.0	1.9	2.5	4	28	31